Proceedings of "Applications of Physics in Mechanical and Material Engineering" (APMME 2024)

Properties of the Superconducting State in $YThH_{12}$ Compound at 60 GPa: Strong-Coupling Approach

M.W. Jarosik*

Division of Physics, Czestochowa University of Technology, al. Armii Krajowej 19, 42-200 Częstochowa, Poland

Doi: 10.12693/APhysPolA.147.204 *e-mail: marcin.jarosik@pcz.pl

Hydrogen-rich ternary compounds have recently emerged as potential candidates for high-temperature superconductors that do not require extremely high pressure conditions. In this work, we provide a quantitative investigation of the thermodynamic properties of the superconducting state in the $YThH_{12}$ compound at a pressure of 60 GPa. Using the Migdal–Eliashberg formalism, we show that the critical temperature of this material is high (T_C = 200.29 K), assuming a Coulomb pseudopotential value of 0.1. In addition, the theoretical framework employed allows for the determination of other key thermodynamic quantities, including the superconducting energy gap, free energy, specific heat, and critical magnetic field. The thermodynamic relationships associated with these parameters differ from those predicted by the Bardeen–Cooper–Schrieffer theory. Our findings indicate that strong-coupling and retardation effects are critical to the superconducting state in this compound, making it inconsistent with a weak-coupling description.

topics: Eliashberg formalism, $YThH_{12}$ superconductor, high-pressure effects, thermodynamic properties

1. Introduction

Superconductivity is a phenomenon that has been known for more than 100 years, but it is still at the center of interest for many researchers. Superconductors with fascinating properties are already used in many fields of science and technology, but new solutions are still being sought to improve their performance. A particularly important parameter is the value of the critical temperature (T_C) at which the material transitions to the superconducting state. For any superconductor currently used in practical applications, the value of T_C is in the cryogenic temperature range, which greatly complicates and increases the cost of its use. For this reason, the development of a material characterized by a critical temperature as high as possible, preferably in the room temperature range, is constantly being pursued.

One way to increase the value of T_C is to subject the superconductor to high pressure (p). The structural changes that occur often improve the superconducting properties of a given material. In addition, some materials that are not superconducting under normal conditions become superconducting under high pressure. A good example is yttrium, which is not superconducting at normal pressure, but becomes superconducting at high pressure of $p = 115$ GPa with T_C = 19.5 K [1]. The effect of pressure on the thermodynamic parameters of the superconducting state induced in the yttrium was analyzed in detail in work [2].

As a further step in raising the critical temperature, Ashcroft [3] proposed in 2004 the possibility of inducing superconductivity in compounds of hydrogen with heavier elements, where the phenomenon of chemical pre-compression makes it possible to significantly reduce the external pressure required to achieve superconductivity. Further studies brought experimental confirmation of these predictions [4, 5], for example, compound YH_6 at 166 GPa showed a transition to a superconducting state at 224 K [6]. With the proposed approach, it was possible to obtain a significant increase in the critical temperature value with a pressure increase that was not too high.

The next goal is to achieve high-temperature superconductivity in hydrides while maintaining relatively moderate pressure conditions. Studies have shown that introducing dopants or molecules into binary hydrides is an effective strategy for lowering the required stabilization pressure. Recently, Chen et al. [7] proposed the introduction of a thorium element into clathrate hexahydrides as a better compressor. Within the framework of theoretical predictions, a number of ternary hydrides have been obtained, the most interesting of which seems to

be the compound $YThH_{12}$ at 60 GPa. Therefore, in the work presented here, we study the thermodynamic parameters of the superconducting state of this compound, taking into account the key role of strong-coupling effects in shaping its superconductivity. The numerical analysis was conducted in the framework of the Eliashberg equations on the imaginary axis [8–10].

It is important to emphasize that Eliashberg's formalism is a major extension of the fundamental theory introduced by Bardeen, Cooper, and Schrieffer (BCS) [11]. It extends the BCS framework by explicitly including the effects of electron–phonon interactions. The starting point of our calculations is the electron–phonon coupling function ($\alpha^2F(\Omega)$). We rely on the function determined with the Quantum ESPRESSO package presented in paper [7]. Based on the above analysis, it was concluded that the key parameters, namely the maximum phonon frequency ($\Omega_{\max}$) and the electron–phonon coupling constant (λ), are 155.8 meV and 3.09, respectively. In the context of Eliashberg's approach, the magnitude of the strong-coupling corrections to BCS predictions is closely related to the value of the key parameter, $k_{\mathrm{B}}T_C/\omega_{\ln}$. The symbol $\omega_{\ln}$ denotes the logarithmic phonon frequency defined as

$$\omega_{\ln} \equiv \exp\left(\frac{2}{\lambda}\int_0^{\Omega_{\max}} \mathrm{d}\Omega \ \ \frac{\alpha^2F(\Omega)}{\Omega}\ln(\Omega)\right), \qquad (1)$$

which in our case is equal to 57.55 meV. In the case of the BCS limit, the Eliashberg function is non-zero only for very high frequency, so that $k_{\mathrm{B}}T_C/\omega_{\ln} \to 0$. For $YThH_{12}$ at 60 GPa, the value of the ratio $k_{\mathrm{B}}T_C/\omega_{\ln}$ is equal to 0.3. This deviation from the BCS limit confirms the need to use more advanced computational methods to accurately calculate the thermodynamic parameters of the superconducting state.

2. The model

From the point of view of numerical computation, it is much easier to solve the Eliashberg equations defined on the imaginary axis. In this approach, it is not necessary to solve complex systems of equations requiring complicated numerical integration, so the calculations require fewer hardware resources and take less time. The results obtained can be analytically extended to the real axis, which requires additional calculations, but is still simpler and faster than solving the Eliashberg equations directly.

The Eliashberg equations, specifically formulated for a half-filled electron band and represented on the imaginary axis, can be succinctly expressed as follows [8]

$$\Delta_n Z_n = \frac{\pi}{\beta}\sum_{m=-M}^{M} \frac{K(n,m) - \mu^*\theta(\omega_c - |\omega_m|)}{\sqrt{\omega_m^2+\Delta_m^2}}\ \Delta_m \qquad (2)$$

and

$$Z_n = 1 + \frac{\pi}{\beta\omega_n}\sum_{m=-M}^{M} \frac{K(n,m)}{\sqrt{\omega_m^2+\Delta_m^2}}\ \omega_m, \qquad (3)$$

where the symbol $\Delta_n \equiv \Delta(\mathrm{i}\omega_n)$ denotes the order parameter and $Z_n \equiv Z(\mathrm{i}\omega_n)$ is the wave function renormalization factor; n-th Matsubara frequency is expressed by $\omega_n \equiv \frac{\pi}{\beta}(2n-1)$, where $\beta \equiv 1/(k_{\mathrm{B}}T)$. The depairing electron effects are parameterized by the Coulomb pseudopotential (μ^*). The symbol θ denotes the Heaviside unit function; ω_c is the cut-off energy and is equal to $5\Omega_{\max}$. The electron–phonon pairing kernel $K(n,m)$ can be defined as follows

$$K(n,m) \equiv 2\int_0^{\Omega_{\max}} \frac{\mathrm{d}\Omega\ \Omega}{(\omega_n-\omega_m)^2+\Omega^2}\ \alpha^2F(\Omega). \qquad (4)$$

3. The numerical results

The number of equations in the system depends on the number of Matsubara frequencies considered. The more equations, the more stable the results are around $T = 0$, but on the other hand, they require much more hardware resources and time to find solutions. In this case, the Eliashberg equations have been solved for 2201 Matsubara frequencies ($M = 1100$) by using the method presented in [12] and [13], and recently tested in [14]. The obtained Eliashberg solutions are stable for $T \geq 30$ K.

Another important parameter within the used model is the Coulomb pseudopotential, which determines the depairing interactions, i.e., those that have a negative effect on the induction of the superconducting state. In the calculations, a typical Coulomb pseudopotential value for systems of this kind, set at $\mu^* = 0.1$, was used. Taking into account the following condition $[\Delta_{m=1}(\mu^*)]_{T=T_C} = 0$, it was demonstrated that the critical temperature value for the $YThH_{12}$ at 60 GPa is 200.29 K.

Figure 1a shows the behavior of the order parameter on the imaginary axis for selected temperature values. It can be seen that the function Δ_m reaches its maximum at $m = 1$. In addition, the successive Matsubara frequencies converge to a constant value more quickly as the temperature increases. Consequently, for temperatures close to absolute zero, it is essential to include a large number of Matsubara frequencies because they significantly influence the equation solutions. In contrast, near the critical temperature, the contribution of higher Matsubara frequencies becomes negligible.

The temperature dependence of the order parameter on the imaginary axis can be easily traced by drawing the curve $\Delta_{m=1}(T)$ (Fig. 1b). The order parameter determines the energy required to break up a Cooper pair and destroy superconductivity. As can be seen, the lower the temperature, the stronger the superconducting state, while it weakens as the temperature increases, with the order parameter

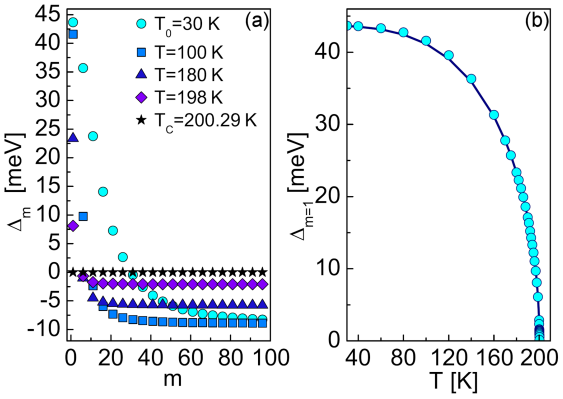

Fig. 1. (a) The order parameter on the imaginary axis for the selected values of temperature. The first 100 values of the Δ_m function are plotted. (b) The influence of temperature on the maximum value of the order parameter. The symbols represent the numerical results. The line was obtained using (5).

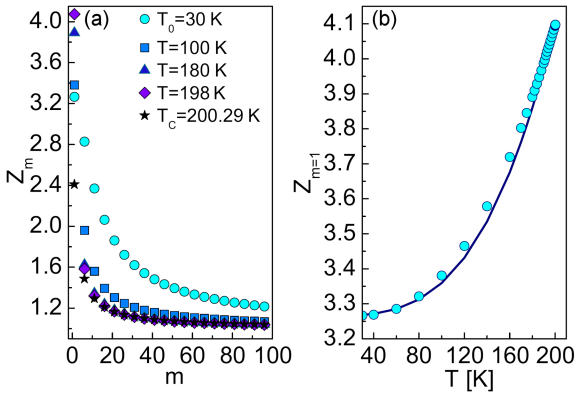

Fig. 2. (a) The wave function renormalization factor on the imaginary axis for the selected values of temperature. The first 100 values of the Z_m function are plotted. (b) The influence of temperature on the maximum value of the renormalization factor. The symbols represent the numerical results. The line was obtained using (6).

reaching zero at the critical temperature, which means that at this point the Cooper pairs decay spontaneously and the superconducting state disappears.

In the case of the $YThH_{12}$ at 60 GPa, the obtained numerical data can be reproduced by the formula

$$\Delta_{m=1}(T) = \Delta_{m=1}(T_0)\sqrt{1-\left(\frac{T}{T_C}\right)^{\kappa}}, \tag{5}$$

where $\Delta_{m=1}(T_0) \approx \Delta_{m=1}(T = 30\ \mathrm{K}) = 43.68$ meV, and $\kappa = 3.15$.

It should be clearly emphasized that within the framework of BCS theory, the value of the function $\Delta_{m=1}(T)$ cannot be correctly determined, since it follows that $[\kappa]_{\mathrm{BCS}} = 3$ [15].

A visualization of the solutions of the Eliashberg equations for the wave function renormalization factor on the imaginary axis is shown in Fig. 2a. As with the order parameter, the function Z_m reaches its maximum value when $m = 1$.

Furthermore, it can be concluded that the effect of temperature on $Z_{m=1}$, although not large, cannot be neglected, as shown in Fig. 2b. In addition, the wave function renormalization factor maintains consistently high values over the entire temperature range studied and increases with temperature. It is worth noting that within the framework of BCS theory, there is $[Z_m]_{\mathrm{BCS}} = 1$.

The apparent increase in the value of the $Z_{m=1}(T)$ function with temperature can be attributed to the significant influence of strong-coupling effects occurring in the $YThH_{12}$ at 60 GPa system. It should be noted that from a physical point of view, the first Matsubara frequency of the wave function renormalization factor determines the ratio of the effective electron mass (m_e^*) to the electron band mass (m_e), i.e., $Z_{m=1} = \frac{m_e^*}{m_e}$.

Interestingly, it is possible to reproduce the numerical results obtained for the wave function renormalization factor using the following formula

$$Z_{m=1}(T) = Z_{m=1}(T_0) + \Big[Z_{m=1}(T_C) - Z_{m=1}(T_0)\Big]\left(\frac{T}{T_C}\right)^{\kappa}, \tag{6}$$

where $Z_{m=1}(T_0) = 3.27$, and $Z_{m=1}(T_C) = 1 + \lambda$.

The determination of the physical value of the order parameter requires a procedure of analytical continuation of the solutions of the Eliashberg equations on the real axis ($\Delta_m \to \Delta(\omega)$). The following formula should be used

$$\Delta(\omega) = \frac{p_1 + p_2\omega + ... + p_r\omega^{r-1}}{q_1 + q_2\omega + ... + q_r\omega^{r-1} + \omega^r}. \tag{7}$$

The values of the parameters p_j and q_j have been determined according to the method presented in the publication [16]. Additionally, it has been assumed $r = 50$.

The results for the order parameter at $T = 30$ K are shown in Fig. 3 (see also [7]). It can be seen that in the low-frequency range, only the real part of the $\Delta(\omega)$ function takes non-zero values. Physically, this means that there are no significant damping effects. Dissipative processes ($\mathrm{Im}[\Delta(\omega)] = 0$) are not observed for low-frequency values. This means that a superconducting condensate is formed by Cooper pairs with an infinite lifetime. Damping effects are important for higher power transmissions and are closely related to phonon emission and absorption, as evidenced by the increase in both $\mathrm{Re}[\Delta(\omega)]$ and $\mathrm{Im}[\Delta(\omega)]$ with increasing frequency.

The next step is to determine the physical value of the order parameter, which can be calculated using the following equation

$$\Delta(T) = \mathrm{Re}\Big[\Delta(\omega{=}\Delta(T), T)\Big]. \tag{8}$$

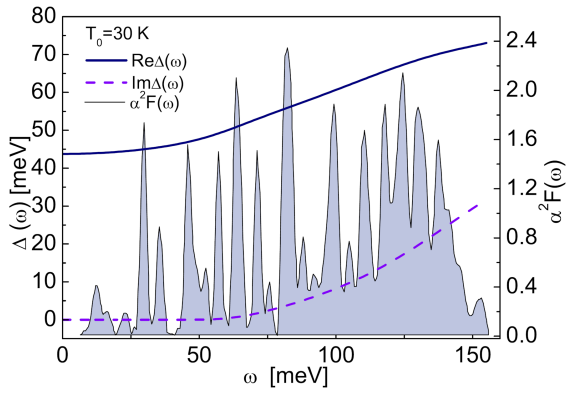

Fig. 3. Real and imaginary part of the order parameter on the real axis for $T = 30$ K. The Eliashberg function [7] is present in the background.

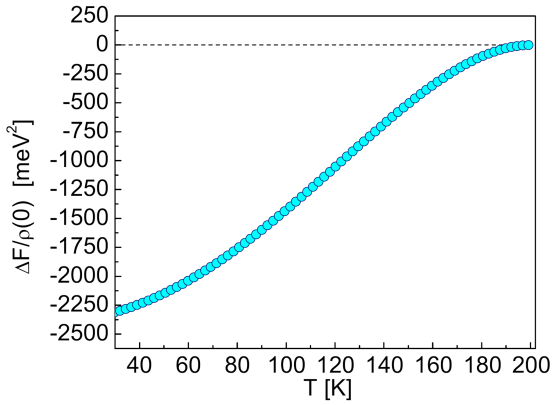

Fig. 4. The free energy difference between the superconducting state and the normal state as a function of temperature.

For $T_0 = 30$ K, the following result has been obtained $\Delta(0) = 47.14$ meV, while $\Delta(0) \equiv \Delta(T_0)$.

The free energy difference between the superconducting and normal state (ΔF) for the $YThH_{12}$ at 60 GPa as a strong electron–phonon coupling system can be calculated by using the expression [17]

$$\frac{\Delta F}{\rho\,(0)} = -\frac{2\pi}{\beta}\sum_{n=1}^{M}\left(\sqrt{\omega_n^2+\Delta_n^2} - |\omega_n|\right) \times\left(Z_n^S - Z_n^N\,\frac{|\omega_n|}{\sqrt{\omega_n^2+\Delta_n^2}}\right), \tag{9}$$

where Z_n^S and Z_n^N denote the wave function renormalization factors for the superconducting (S) and normal (N) states, respectively, while $\rho(0)$ is the electron density of states at the Fermi level. In Fig. 4, the dependence of ΔF on the temperature has been plotted. In the context of the physical interpretation, the presence of negative values of ΔF provides convincing evidence that the superconducting state remains stable below the critical temperature.

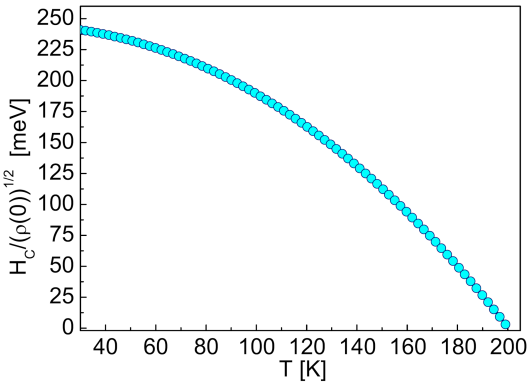

Fig. 5. The thermodynamic critical field as a function of temperature.

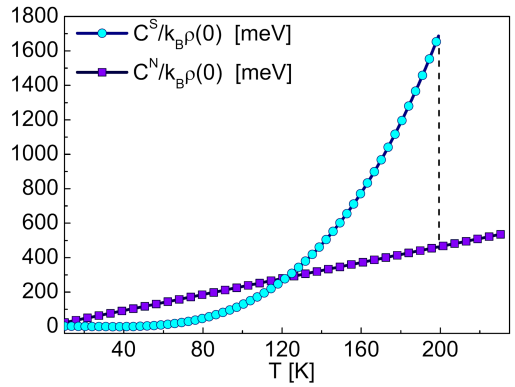

Fig. 6. The dependence of the specific heat in the superconducting and normal state on the temperature.

In the next step, the dependence of the thermodynamic critical field on the temperature was calculated using the following formula (cgs units)

$$\frac{H_C}{\sqrt{\rho\,(0)}} = \sqrt{-8\pi\,[\Delta F/\rho\,(0)]}. \tag{10}$$

The temperature dependence of $H_C/\sqrt{\rho(0)}$ has been shown in Fig. 5. As can be easily seen, the thermodynamic critical field reaches its maximum value at T_0 and decreases with increasing temperature, finally reaching zero at T_C. The result can be interpreted in such a way that the external critical field destroys the superconducting state and its highest value can be applied in the lowest temperature range.

The specific heat difference between superconducting and normal state ($\Delta C{=}C^S{-}C^N$) is given by

$$\frac{\Delta C\,(T)}{k_{\mathrm{B}}\,\rho\,(0)} = -\frac{1}{\beta}\frac{\mathrm{d}^2\,[\Delta F/\rho\,(0)]}{\mathrm{d}\,(k_{\mathrm{B}}T)^2}. \tag{11}$$

The easiest way to estimate the specific heat of the normal state is to use the formula

$$\frac{C^N\,(T)}{k_{\mathrm{B}}\,\rho\,(0)} = \frac{\gamma}{\beta}, \tag{12}$$

where the Sommerfeld constant is given by $\gamma \equiv \frac{2}{3}\pi^2(1+\lambda)$. The relationship between temperature and specific heat for both the superconducting and normal states is illustrated in Fig. 6. The pronounced discontinuity associated with the phase transition between the superconducting and normal states is observed precisely at the critical temperature, which is marked by the vertical dashed line.

The thermodynamic functions determined in this work allow for the calculation of values of characteristic dimensionless ratios

$$R_\Delta \equiv \frac{2\Delta(0)}{k_B T_C} = 5.46, \tag{13}$$

$$R_C \equiv \frac{\Delta C(T_C)}{C^N(T_C)} = 2.70, \tag{14}$$

$$R_H \equiv \frac{T_C C^N(T_C)}{H_C^2(0)} = 0.133. \tag{15}$$

It should be noted that the parameters R_Δ, R_C and R_H in the framework of BCS theory are universal constants and for any superconductor they take on equal values of 3.53, 1.43, and 0.168, respectively [14, 17].

4. Conclusions

In the present study, a quantitative analysis of the superconducting state parameters in the compound $YThH_{12}$ at 60 GPa was carried out using the Eliashberg formalism. The study showed that this superconductor has a high critical temperature of $T_C = 200.29$ K, which is a significant advantage over similar binary hydride systems that require much higher pressures to achieve similar T_C values. The results obtained confirm the effectiveness of introducing an additional heavy element as a structural compressor, which may be an effective strategy for designing new high-temperature superconductors.

In addition, a detailed analysis of the dimensionless parameters showed significant deviations from the predictions of BCS theory. The values of the coefficients $R_\Delta = 5.46$, $R_C = 2.70$, and $R_H = 0.133$ are distinctly different from the classical BCS predictions, which clearly indicates the strongly coupled nature of this superconductor. In addition, the ratio of the effective electron mass (m_e^*) to the electron band mass (m_e) reaches a maximum value of 4.09 at the critical temperature, implying a more than fourfold increase in the effective mass due to the intense interaction of the electrons with the vibrations of the crystal lattice.

The above results, combined with significant retardation effects, clearly prove that $YThH_{12}$ at 60 GPa cannot be correctly described within the framework of classical BCS theory. Its analysis requires the use of more advanced theoretical models, such as Eliashberg's formalism, which takes into account the influence of strong electron–phonon couplings and delay effects. The results not only shed new light on superconductivity in hydride systems, but also point the way for further research on materials capable of achieving superconductivity under milder pressure conditions, which may be crucial for future technological applications.

References

[1] J.J. Hamlin, V.G. Tissen, J.S. Schilling, *Physica C* **451**, 82 (2007).

[2] M.W. Jarosik, I.A. Wrona, A.M.Duda, *Solid State Commun.* **219**, 1 (2015).

[3] N.W. Ashcroft, *Phys. Rev. Lett.* **92**, 187002 (2004).

[4] D. Duan, Y. Liu, F. Tian, X. Huang, Z. Zhao, H. Yu, B. Liu, W. Tian, T. Cui, *Sci. Rep.* **4**, 6968 (2014).

[5] M. Somayazulu, M. Ahart, A.K. Mishra, Z.M. Geballe, M. Baldini, Y. Meng, V.V. Struzhkin, R.J. Hemley, *Phys. Rev. Lett.* **122**, 027001 (2019).

[6] I.A. Troyan, D.V. Semenok, A.G. Kvashnin et al., *Adv. Mater.* **33**, 2006832 (2021).

[7] W. Chen, T. Ma, Z. Huo, H. Yu, T. Cui, D. Duan, *Phys. Rev. B* **109**, 224505 (2024).

[8] G.M. Eliashberg, *Soviet. Phys. JETP* **11**, 696 (1960).

[9] J.P. Carbotte, *Rev. Mod. Phys.* **62**, 1027 (1990).

[10] R. Szczęśniak, *Acta Phys. Pol. A* **109**, 179 (2006).

[11] J. Bardeen, L.N. Cooper, J.R. Schrieffer, *Phys. Rev.* **106**, 162 (1957).

[12] I.A. Wrona, P. Niegodajew, Y. Li, A.P. Durajski, *npj Comput. Mater.* **10**, 289 (2024).

[13] I.A. Wrona, P. Niegodajew, A.P. Durajski, *Mater. Today Phys.* **46**, 101499 (2024).

[14] I.A. Wrona, R. Szczęśniak, A.P. Durajski, *J. Phys. Chem. C* **128**, 9247 (2024).

[15] H. Eschrig, *Theory of Superconductivity a Primer*, 2001.

[16] K.S.D. Beach, R.J. Gooding, F. Marsiglio, *Phys. Rev. B* **61**, 5147 (2000).

[17] J. Bardeen, M. Stephen, *Phys. Rev.* **136**, A1485 (1964).